ARTICLE

Fabrication of Complex Metallic Nanostructures by Nanoskiving

Qiaobing Xu, Robert M. Rioux, and George M. Whitesides*

Department of Chemistry and Chemical Biology, Harvard University, 12 Oxford Street, Cambridge, Massachusetts 02138

ABSTRACT This paper describes the use of nanoskiving to fabricate complex metallic nanostructures by sectioning polymer slabs containing small, embedded metal structures. This method begins with the deposition of thin metallic films on an epoxy substrate by e-beam evaporation or sputtering. After embedding the thin metallic film in an epoxy matrix, sectioning (in a plane perpendicular or parallel to the metal film) with an ultramicrotome generates sections (which can be as thin as 50 nm) of epoxy containing metallic nanostructures. The cross-sectional dimensions of the metal wires embedded in the resulting thin epoxy sections are controlled by the thickness of the evaporated metal film (which can be as small as 20 nm) and the thickness of the sections cut by the ultramicrotome; this work uses a standard 45° diamond knife and routinely generates slabs 50 nm thick. The embedded nanostructures can be transferred to, and positioned on, planar or curved substrates by manipulating the thin polymer film. Removal of the epoxy matrix by etching with an oxygen plasma generates free-standing metallic nanostructures. Nanoskiving can fabricate complex nanostructures that are difficult or impossible to achieve by other methods of nanofabrication. These include multilayer structures, structures on curved surfaces, structures that span gaps, structures in less familiar materials, structures with high aspect ratios, and large-area structures comprising two-dimensional periodic arrays. This paper illustrates one class of application of these nanostructures: frequency-selective surfaces at mid-IR wavelengths.

KEYWORDS: nanoskiving · microtome sectioning · nanofabrication · manipulation · nonplanar · nanophotonics

This article describes several routes to fabricate complex metallic nanostructures by nanoskiving. The origin of the term "nanoskiving" is in the word "skiving" (a procedure used to cut thin slices from a thicker bulk material).[1] Nanoskiving combines deposition of thin films of metal on an epoxy substrate, with sectioning of an epoxy block (containing the thin metal films) using an ultramicrotome. It is experimentally simple and requires little in the way of facilities (for example, access to a cleanroom or a high-resolution e-beam writer is unnecessary). It is applicable to many classes of structures and materials with which conventional methods of nanofabrication (*e.g.*, EUV or X-ray photolithography, e-beam lithography (EBL), focused ion-beam (FIB)) fail. The technique described in this paper has the ability both to generate "master" structures (that is, it does not require the nanostructures to be written in a separate step using a technique such as e-beam writing or FIB) and to "manufacture" (that is to make hundreds of copies of a nanostructure). It thus provides a new capability to nanofabrication. In this technique, we embed thin (20–100 nm) metal structures in an epoxy substrate and section the resulting structure into thin (50–1000 nm) slabs in a plane perpendicular (or parallel) to the thin metal film using an ultramicrotome (Figure 1). The thickness of the deposited metal film and the thickness of the sections cut by the ultramicrotome determine the cross-section of the metal structures in these epoxy sections.

Conventional top-down techniques to generate nanoscale structures and nanostructured materials include photolithography[2–5] and scanning-beam lithography (*e.g.*, electron beam and FIB lithography).[6–9] Although these techniques are useful, versatile, and highly developed, they also have limitations: high capital and operating costs, limited availability of the facilities required to use them, an inability to fabricate structures on nonplanar surfaces, and restrictions on the classes of materials that can be fabricated with them caused by concerns for cross-contamination (especially in microelectronics fabrication). An additional limitation of the scanning-beam methods is that they are serial. Fabrication of three-dimensional (3D) nanostructures still remains a challenge and often requires complicated techniques such as multiphoton absorption lithography; this technique is a serial process and is limited to minimal feature sizes of 100 nm.[10] Nanoscience and nanotechnology would benefit from new, low-cost techniques to fabricate electrically and optically functional structures with

See the accompanying Perspective by Rogers on p 151.

*Address correspondence to gwhitesides@gmwgroup.harvard.edu.

Received for review August 15, 2007 and accepted September 28, 2007.

Published online October 31, 2007.
10.1021/nn700172c CCC: $37.00

© 2007 American Chemical Society

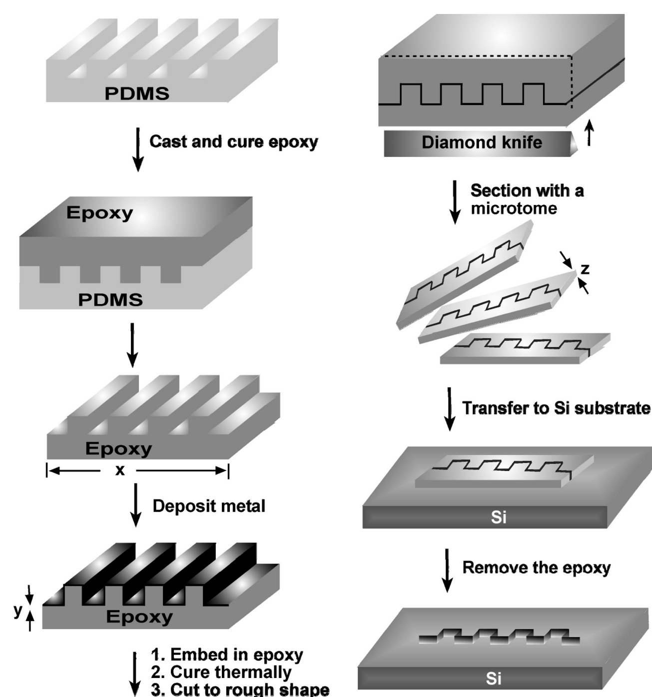

Figure 1. The procedure used to fabricate metallic nanostructures by nanoskiving. This method begins with the replication of a flat or topographically patterned poly(dimethylsiloxane) (PDMS) surface in epoxy, followed by the deposition of thin metallic films by e-beam evaporation or sputtering. The topography of the original template determines the dimension along the *x*-direction. The thickness of the evaporated metal film determines the dimension in the *y*-direction and can be as small as 20 nm for gold. After embedding the thin-metal film in more epoxy and curing, sectioning with an ultramicrotome produces sections in the *z*-direction with a thickness as small as 50 nm using a standard 45° diamond knife. After sectioning, we transfer the epoxy section to a silicon substrate and remove the epoxy with an oxygen plasma. All cross-sections in this paper refer to the *y*- and *z*-dimensions defined above.

dimensions of tens of nanometers, even if (or perhaps especially if) these techniques have a different range of application than do photolithography and scanning-beam lithography.[11−13]

Exploration of unconventional methods for nanofabrication has, of course, generated a number of new techniques:[13] these include soft lithography (in a number of embodiments),[12−28] templated electrodeposition,[29,30] nanoimprint lithography (NIL),[31−34] step-and-flash imprinting lithography,[35,36] edge lithography,[37−42] and scanning-probe lithographies (SPL),[43−47] including dip-pen lithography (DPL).[45,48−51] Recently, we described a method[40,52−54] that we call "nanoskiving" to fabricate nanoscale structures based on thin metal film deposition and sectioning by microtomy.[55] This paper describes routes that use nanoskiving to fabricate complex nanostructures. These routes include (i) nanoskiving in a direction perpendicular to a patterned substrate, (ii) nanoskiving in a direction parallel to a patterned substrate, and (iii) positioning and stacking of the epoxy slabs generated by nanoskiving. The work presented here introduces new capabilities—fabrication of new nanostructures, positioning these nanostructures on unconventional substrates, and stacking the slabs containing the nanostructures to form quasi-3D structures—which we have not described in previous publications.[40,52−54]

Nanoskiving is not competitive with photolithography or scanning-beam methods for making the multilayer, registered structures required for microelectronic devices. In particular, it does not have the layer-to-layer dimensional stability required in multilayer registered structures. Instead, it provides a simpler and substantially more accessible and practical alternative to these methods for making simple nanostructures, and we believe that it will allow nonspecialists (*i.e.*, biologists, chemists, and materials scientists) to fabricate functional nanostructures for research in materials science, surface science, optics, and biomedicine. The method we describe here is especially useful for single-layer structures (*e.g.*, those useful in photonics), for nanostructures on curved and nonplanar surfaces (*e.g.*, suspended wires and wires supported on the surface of small lenses or cylinders), and for structures fabricated in materials that are difficult to manipulate using conventional methods.

RESULTS AND DISCUSSION

Methods of Nanoskiving. "Nanoskiving" is the name we have given to a technique for the fabrication of nanostructures by combining deposition of thin films using physical vapor methods and sectioning with an ultramicrotome. The ultramicrotome is used extensively for the preparation of thin samples for imaging with optical or electron microscopy.[56,57] Figure 2A is a photograph of an ultramicrotome system manufactured by Leica Microsystems. The operation of an ultramicrotome is based on the controlled mechanical advance of a sample arm that holds the sample to be sectioned. The mechanism that advances the arm comprises a stepping motor and spindle; a lever transforms micrometer-increment steps of the sample arm into nanometer-increment steps of the sample relative to a stationary knife. Proper design of the lever and its bearing assembly ensures high stability and step increments as small as 1 nm.[58] During the down-stroke of the sample arm, the sample is forced against the edge of the diamond knife. The resulting section separates as a thin slab from the face of the sample block and floats from the backside of the knife onto the surface of water filling the knife trough. A microtome can generate polymer sections as thick as ~10 μm or more with a rotary microtome system[59] and as thin as 20 nm with an ultrasonic 35° diamond knife mounted to an ultramicrotome.[60]

Figure 1 outlines the procedure for fabricating embedded metal nanostructures by nanoskiving: this procedure generates step-shaped nanostructures. We obtained a patterned epoxy substrate by curing an epoxy prepolymer (Araldite 502) overnight at 70 °C against a topographically patterned poly(dimethylsiloxane)

(PDMS) substrate. The low free energy of the surface of PDMS enabled the two polymers to be separated easily. We used Araldite 502 epoxy to embed the thin metal films or structures,[61,62] because this polymer has (i) mechanical properties appropriate for microtome sectioning at room temperature;[40] (ii) the physical properties required to provide support for the nanostructures that are formed upon sectioning (this support allows these sections to be manipulated); (iii) rapid rates of etching in an oxygen plasma, so it can be removed easily; and (iv) good adhesion to gold *without* a titanium adhesion layer.[63] Other polymers may be more appropriate than Araldite 502 for specific applications.

After replicating a PDMS master in epoxy, we deposited a thin gold film (10–100 nm) directly onto the epoxy, without a titanium adhesion layer, using e-beam evaporation. We cut this epoxy-supported metal film in thin strips (~1 mm width × ~5 mm length) using a razor blade and placed these strips into a flat embedding mold. After filling the embedding mold with more epoxy of the same kind, we cured the epoxy for 12 h at 70 °C. After removing the cured polymer from the mold, we trimmed its face to dimensions of 0.5 mm height × 0.5 mm width using a razor blade under a stereomicroscope, mounted it on the ultramicrotome, and sectioned it with a diamond knife with a wedge angle of 45°. There are several types of commercially available diamond knives for use with microtomy,[60] each suited for specific applications. In this work, we used a 45° diamond knife (Diatome USA, Hatfield, PA) to generate epoxy slabs with a thickness between 50 and 1000 nm. After sectioning, the slabs floated away from the edge of the diamond knife onto the surface of water filling the sample-collecting reservoir. Sectioning requires about 3 s for a slice with areal dimensions of 0.5 mm × 0.5 mm, and with a 50-nm thickness; sectioning can, thus, generate a large number of slabs rapidly (we have made 200 in 10 min).

We used two methods to transfer these thin epoxy slabs from the surface of the water onto a solid substrate (*e.g.*, a TEM grid or a silicon wafer) (Figure 2B,C). The first method involves the transfer of an epoxy cross-section slab from the surface of the water to a substrate using a 2-mm diameter collection loop. The thin film of water on the collection loop supported the slab of epoxy containing the embedded gold nanostructures. We brought the collection loop into physical contact with a substrate (*i.e.*, silicon substrate or TEM grid) and wicked away the water using a paper tissue; this procedure left the epoxy section supported on the substrate.

The second method relies on the direct transfer of the epoxy slab from the surface of water onto a substrate by submerging the substrate (a silicon wafer in Figure 2C) directly below the floating epoxy section(s) and pulling the substrate toward the section(s) in such a way that it (or they) settle(s) on the substrate. Figure

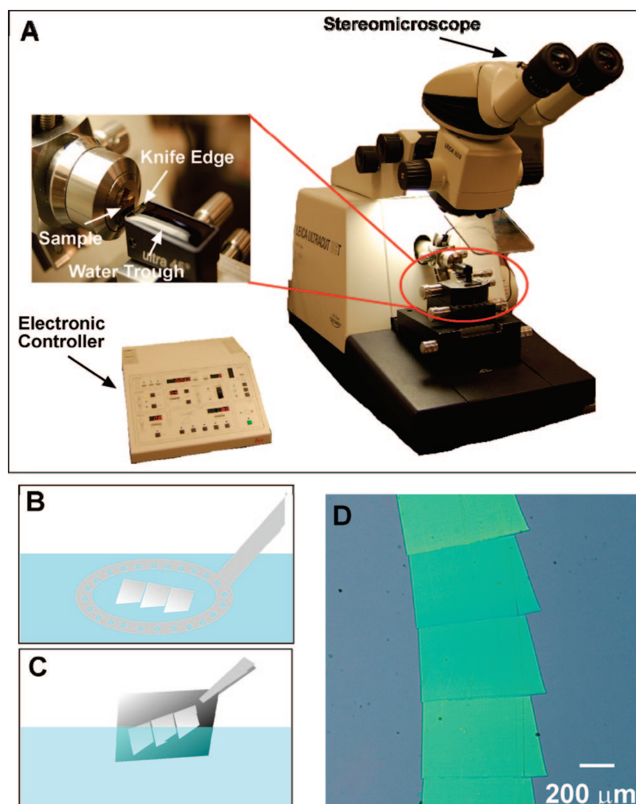

Figure 2. (A) Photograph of an ultramicrotome and close-up photograph of the sample and diamond knife mount. The specimen in this research, for example, a gold film embedded in epoxy, is secured (by a set screw) to the specimen arm which mechanically advances forward in nanometer increments. The motion generates an epoxy section with the completion of each down-stroke; this section floats on the surface of water filling the knife trough. (B,C) Schematic diagrams of the two methods used for the collection of slabs and for the further manipulation of these sections (*e.g.*, positioning on a substrate). Epoxy sections floating on the surface of water are collected with a loop which supports a thin film of water and holds the sample by capillarity or by the "direct capture" of the epoxy film onto a substrate (piece of silicon wafer shown in panel C). (D) Bright-field optical microscopy image of multiple sections using white light illumination. Capillary interactions between epoxy sections on the surface of a SiO_2/Si(100) substrate allow the formation of self-assembled "rafts" of sections using the direct-capture method.

2D is a bright-field optical micrograph of an ordered assembly of multiple thin sections of epoxy containing embedded metallic nanostructures supported on a SiO_2/Si(100) substrate, illuminated with white light. The uniformity of the color (determined by optical interference at the two faces of the slab) of the individual thin-film slabs (Figure 2D) demonstrates the high uniformity (in thickness) obtained with microtomy.[64] The self-assembly of the thin-film epoxy slabs is a route to the fabrication of large-area patterned arrays.[53,65]

Fabrication of Complex Nanostructures Using Topographically Patterned Substrates as a Template. ***Sectioning Perpendicular to the Plane of the Surface.*** Figure 3 shows two types of high-aspect-ratio, free-standing, continuous 3D nanostructures fabricated by nanoskiving epoxy replicas of topographically patterned templates. In the first example, the structure is a replica of photolithographically patterned 1-μm wide lines with 1 μm separation (Figure

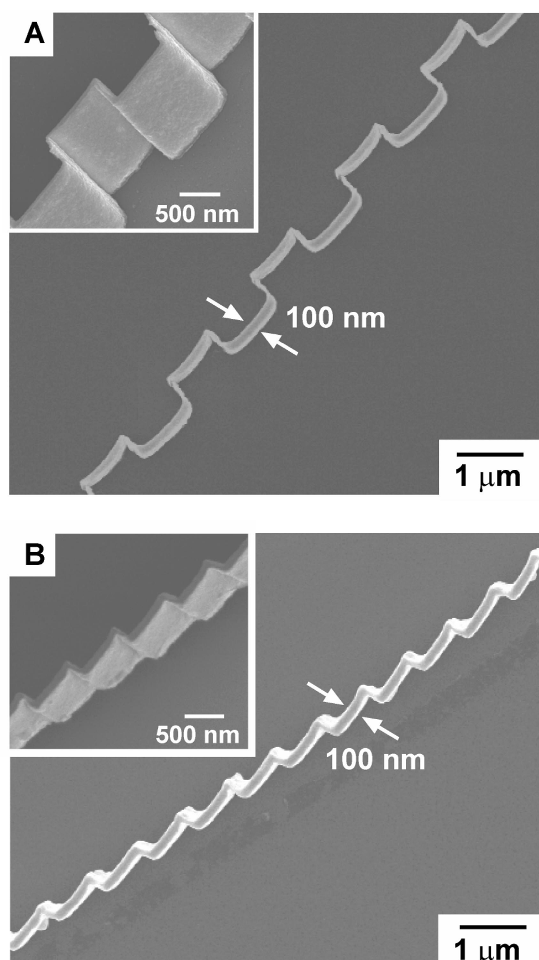

Figure 3. Fabrication of high-aspect-ratio nanostructures by nanoskiving. The structures shown here have an aspect ratio of 10. The aspect ratio is defined as ratio of the height of the structure(s) determined by sectioning with a ultramicrotome (*z*) to the width of the nanostructure(s) determined by the thickness of the evaporated metal film (*y*). (A) SEM image of a continuous gold nanostructure after sputtering a 100-nm thick gold film on an epoxy replica of photolithographically patterned 1-μm wide parallel lines separated by 1 μm. After embedding the gold-covered epoxy replica in more epoxy of the same kind, we removed 1000-nm thick sections with an ultramicrotome. (B) SEM image of a gold nanostructure after sputtering a 100-nm thick gold film on an epoxy replica of a blazed diffraction grating. After embedding the gold-covered epoxy replica in more epoxy of the same kind, we removed 1000-nm thick sections with an ultramicrotome. The inset clearly demonstrates the high aspect ratio of the sample. In both panels, the deposition of gold by sputtering rather than e-beam evaporation ensures metal coverage on all surfaces including sidewalls. The epoxy sections containing the embedded nanostructures are supported on SiO_2/Si(100) substrates, followed by removal of the embedding epoxy with an oxygen plasma.

3A), generated by standard methods of soft lithography.[14] Figure 3B shows a zig-zag-shaped nanostructure sectioned using a gold-coated epoxy replica of a blazed glass diffraction grating. After replica molding the surfaces in PDMS and again in epoxy, we deposited a 100-nm layer of gold by sputtering on the topographically patterned epoxy. The non-collimated flux of the metal atoms in sputtering (due to their multiple collisions in the high-pressure environment of the sputtering chamber) enables metal coverage on sidewalls and forms continuous coatings. Following the procedure outlined in Figure 1, we embedded these metal-coated surfaces in more epoxy and sectioned into slabs (1000-nm thickness) with an ultramicrotome. These structures have an aspect ratio (defined as the ratio of the height of the structure(s) determined by sectioning with an ultramicrotome (*z*) to the width of the nanostructure(s) determined by the thickness of the evaporated metal film (*y*)) of 10. After supporting the epoxy slabs on a SiO_2/Si(100) substrate, we removed the epoxy with an oxygen plasma to expose the gold nanostructures.

Sectioning Parallel to the Plane of the Surface. We previously demonstrated sectioning in a plane parallel to a patterned substrate to fabricate large-area arrays of nanostructures with a shape defined by the original, photolithographically generated template.[53,54] It is also possible using this geometry to fabricate parallel nanowires by a similar procedure using, as a template, a pattern of 2-μm wide lines with 2-μm spacing, generated by photolithography (Figure 4A). After replication in PDMS using standard soft lithography procedures, we molded the PDMS stamp of the photolithographically generated lines in epoxy, deposited a 40-nm thick layer of gold uniformly onto the epoxy replica by sputtering, and embedded the resulting metal structures in more epoxy of the same kind. We sectioned the sample block in a direction parallel (rather than perpendicular, as shown in Figure 3A) to the patterned surface; this orientation generated epoxy slabs containing embedded parallel nanowires. Figure 4B is a scanning electron microscopy (SEM) image of a series of parallel gold nanowires on a SiO_2/Si(100) substrate. The nanowires have a cross-section dimension of 40 nm (*y*) × 70 nm (*z*). The template (2-μm line separated by 2 μm; generated by photolithography using a chrome mask as a master pattern generator) determined the spacing between nanowires.

Multilayer Thin Films by Deposition of Alternating Layers of Au and SiO_2 onto Flat Epoxy Substrates: Templated Complex Nanostructures by Shadow Deposition onto Epoxy Replica Substrates. ***Deposition of Multilayer Films.*** We fabricated composite (*e.g.*, multilayer) nanostructures by varying the composition of the metal(s)/metal oxides evaporated during deposition. For example, we deposited alternating layers of Au (20 nm) and SiO_2 (20 nm) on a SiO_2/Si(100) substrate by sputtering (Figure 5A). We deposited the first layer of gold directly onto the silicon substrate because the adhesion between these two surfaces in the absence of an adhesion layer is poor. After sputtering, we cured (70 °C for 12 h) an epoxy layer (2-mm thick) to the last gold layer. Insertion of a razor blade between the epoxy and surface of the silicon substrate caused the two surfaces to separate and left the silicon substrate exposed, with the alternating Au and

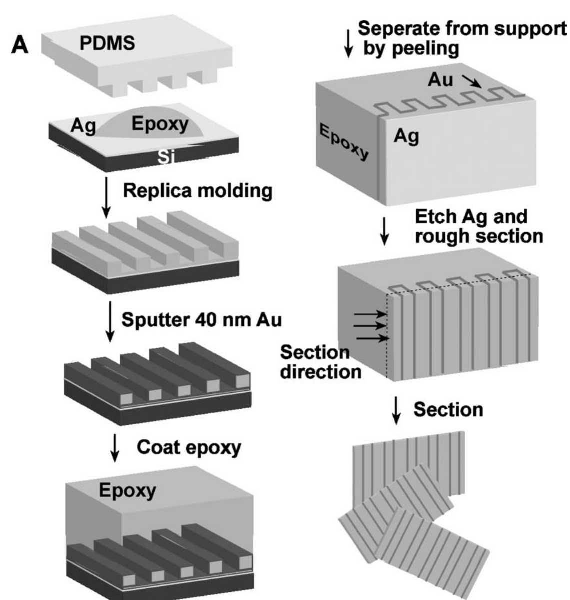

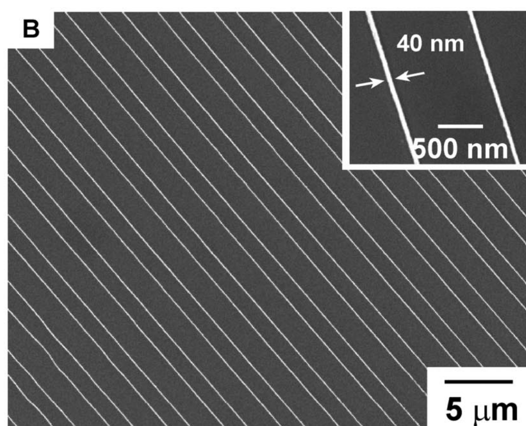

Figure 4. (A) Schematic illustration of the method used to fabricate parallel gold nanowires by sectioning in a plane parallel to the line-patterned surface. (B) SEM image of the gold nanowires with a cross-section of 40 nm (y) × 70 nm (z) (Figure 1) supported on a SiO_2/Si(100) substrate after removal of the epoxy with an oxygen plasma. The inset is a high-magnification SEM image of a gold nanowire with a width of 40 nm. A larger version of the schematic—revealing more detail—is in the Supporting Information (Figure S1).

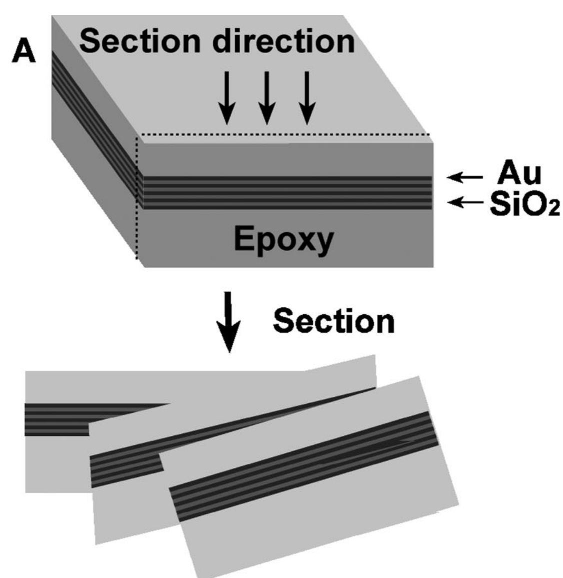

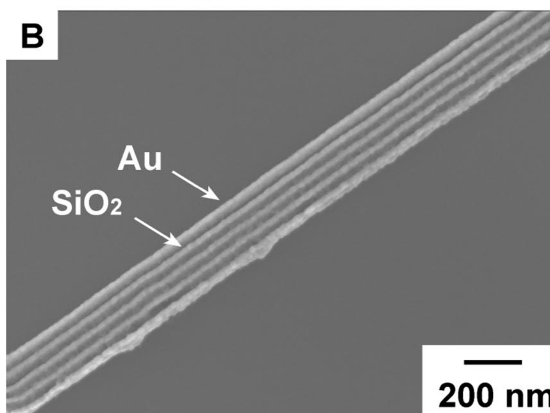

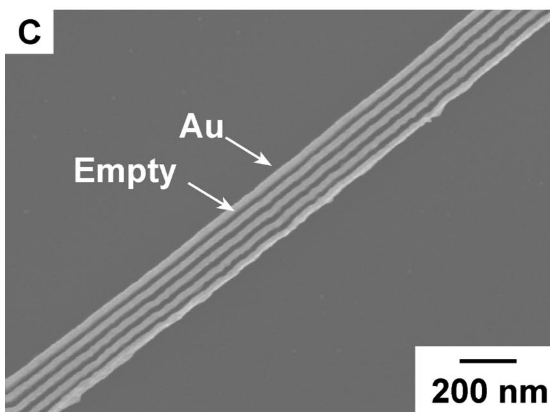

Figure 5. (A) Schematic illustration of the fabrication of composite, multilayer nanostructures by multilayer thin-film deposition and sectioning with an ultramicrotome in a plane perpendicular to the plane of the metal film. (B) SEM image of composite nanowires with alternating gold and SiO_2 layers on a SiO_2/Si(100) substrate after removal of the epoxy with an oxygen plasma. (C) SEM image of the silicon-supported parallel gold nanowires after removal of the 20-nm-thick SiO_2 spacer layers by RIE with CF_4.

SiO_2 layers attached to the epoxy. We embedded the epoxy-backed multilayer film in more epoxy by the procedure outlined in Figure 1. After microtome sectioning (70-nm thickness) and collecting, we supported the epoxy slabs on a SiO_2/Si(100) substrate (Figure 5B). We removed the epoxy film with an oxygen plasma and the silica layer between the gold wires using reactive-ion etching (RIE) with CF_4. Figure 5C is an SEM image of parallel gold nanowires separated by 20 nm generated by this procedure. We investigated the surface of nanowires after sectioning with the ultramicrotome and epoxy removal. The surface exposed after sectioning was rough, suggesting that the thin metal films tear upon sectioning (Supporting Information, Figure S2). The influence of thermal annealing on the surface roughness of the nanowire is included in the Supporting Information. We found that the surface roughness decreases after annealing at ~170 °C, although the wires become

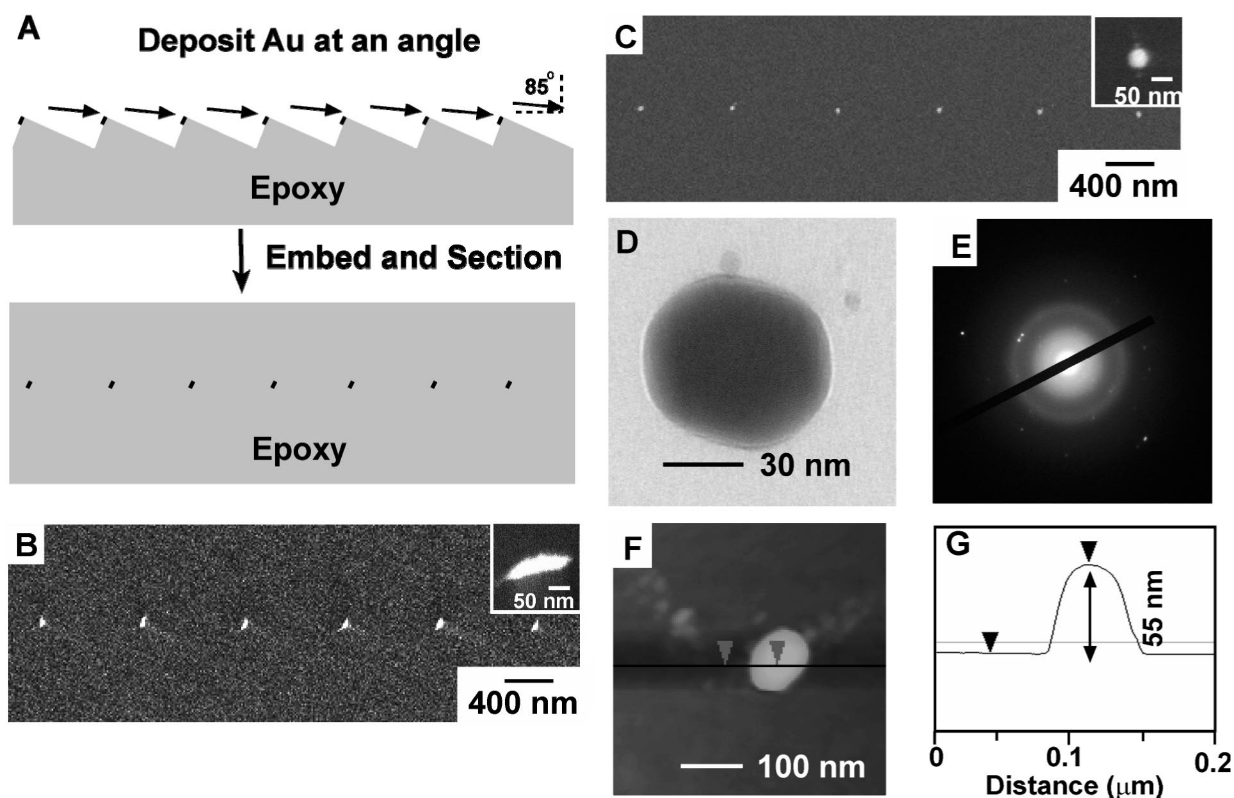

Figure 6. (A) Schematic illustration of the method used to fabricate Au nanoparticles using an epoxy replica of a blazed diffraction grating. Using shadow evaporation, we selectively formed thin wires of gold on the ridges of the grooves of a grating of an epoxy replica. (B) SEM image of the ellipsoidal-shaped gold nanostructures on a SiO_2/Si substrate after removal of the epoxy by oxygen plasma. (C) SEM image of the same gold nanostructures after annealing in air at 500 °C for 2 h. The inset demonstrates that the ellipsoidal-shaped nanostructures become spherical after the annealing step. The distance between these particles (800 nm) is defined by the pitch of the blazed diffraction grating used as the template. (D) TEM image of a single annealed nanoparticle with a diameter of ~60–70 nm. (E) SAED pattern of the annealed nanoparticle in panel D, demonstrating that the nanoparticle is polycrystalline. (F) A tapping-mode AFM image of an annealed nanoparticle, demonstrating that it has a diameter of ~60–70 nm. (G) A cross-section scan of a nanoparticle with AFM, demonstrating that the height of the nanoparticle is ~50–60 nm.

visibly thinner at irregular intervals along the length of the nanowire. At temperatures greater than 250 °C, the wires break at the location of the thinning of the nanowire.

Deposition of Metal on Selected Areas of a Topographically Patterned Epoxy Substrate by Shadow Evaporation. We fabricated arrays of gold nanoparticles on a SiO_2/Si(100) substrate by shadow evaporation of a 10-nm thick film of gold onto the ridges of the grooves of an epoxy replica of a commercial blazed diffraction grating (Figure 6A). We re-embedded the gold-coated epoxy replica in more epoxy, sectioned with an ultramicrotome, and transferred the embedded gold nanoparticles onto a SiO_2/Si(100) substrate. Figure 6B is an SEM image of the ellipsoidal-shaped gold nanoparticles supported on a SiO_2/Si(100) substrate after removal of the epoxy with an oxygen plasma. Figure 6C is an SEM image of the same nanoparticles (with epoxy removal) after annealing in air at 500 °C for 2 h in a convection oven. Prior to annealing, the average length of the Au ellipsoidal-shaped structures was 150 nm (Figure 6B, inset); the particle-to-particle separation was 800 nm. After annealing, the particles had a spherical cross-section with a diameter of ~60–70 nm, as measured by transmission electron microscopy (TEM) (Figure 6D). The selected-area electron diffraction (SAED) pattern had very weak diffraction spots with very diffuse rings, demonstrating that the annealed particle was glassy or polycrystalline (Figure 6E). A tapping-mode atomic force microscopy (AFM) image of the annealed nanoparticle confirmed the particle diameter determined by electron microscopy (Figure 6F). The height of the particle determined from a cross-section of the particle in Figure 6F was ~50–60 nm (Figure 6G). The pitch of the blazed diffraction grating determined the ultimate spacing between the particles.

Figure 7A outlines a procedure to fabricate arrays of open square ("U-shaped") nanostructures by shadow evaporation from three directions with the sample mounted 60° from the plane for line-of-sight evaporation onto three edges of the square template. After sectioning (100-nm thickness), we supported the section on a SiO_2/Si(100) substrate and removed the epoxy with an oxygen plasma. Figure 7B is an SEM image of an array of gold U-shaped nanostructures supported on a Si(100)/Si substrate after the removal of the epoxy. The

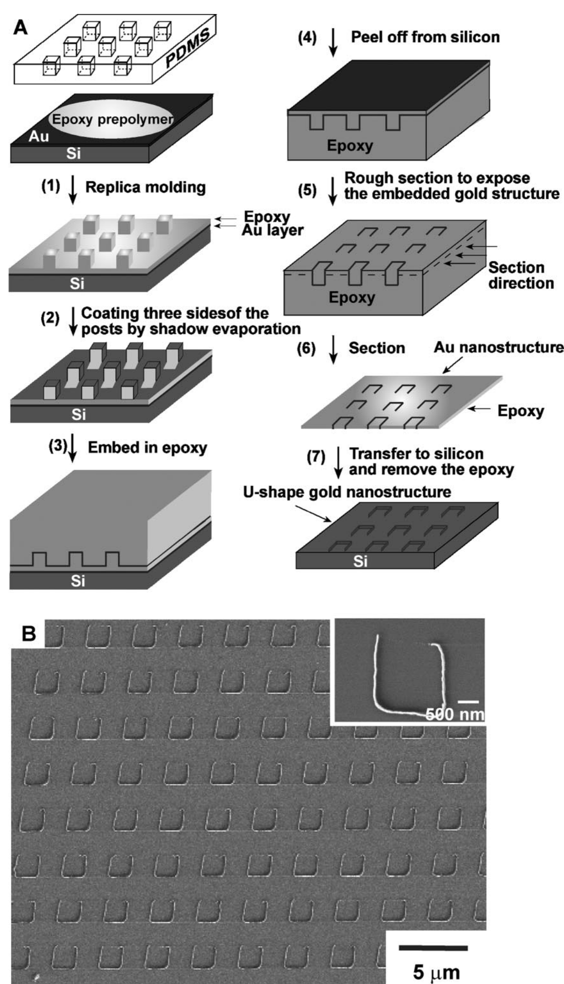

Figure 7. (A) Schematic illustration of the procedure used to fabricate arrays of U-shaped nanostructures on a SiO_2/Si(100) substrate. The U-shaped structures are fabricated by selective shadow deposition of gold by electron-beam evaporation on three corners of the square template replica in epoxy. (B) SEM image of an array of gold U-shaped nanostructures deposited on SiO_2/Si(100). After embedding the gold-covered epoxy replica in more epoxy of the same kind, we removed 100-nm thick sections with an ultramicrotome. The epoxy sections containing the embedded nanostructures are supported on silicon substrates, followed by removal of the embedding epoxy with an oxygen plasma. A larger version of the schematic—revealing more detail—is in the Supporting Information (Figure S3).

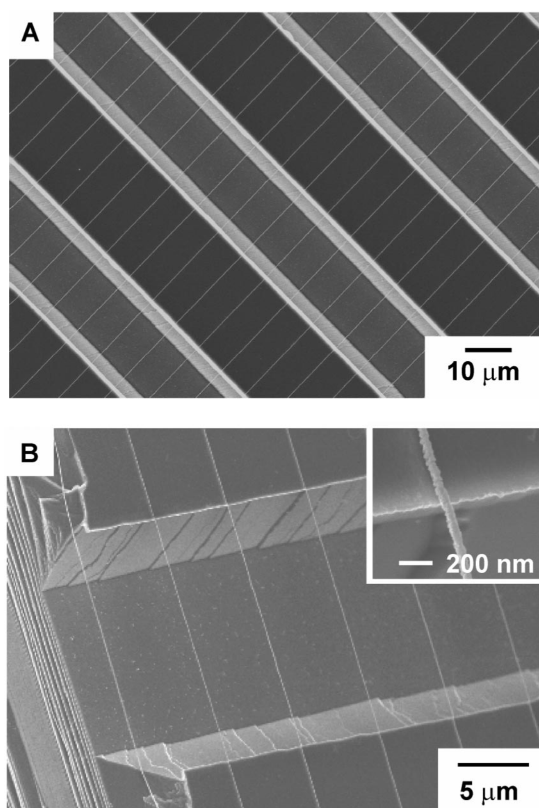

Figure 8. (A) SEM image of parallel nanowires over 20-μm wide "truncated-V"-shaped trenches etched in a Si(100) surface. We removed the epoxy with an oxygen plasma after draping the epoxy section across the trench. (B) SEM image of parallel Au nanowires draped across a single 20-μm wide truncated-V-shaped trench previously etched in a Si(100) substrate with KOH. We removed the epoxy with an oxygen plasma after draping the epoxy section across the trench. The inset is a magnified SEM image of a single Au nanowire with a cross-section of 40 nm (y) × 70 nm (z) at the edge of the gap etched into the Si surface.

inset of Figure 7B shows that the U-shaped structure does not have the exact shape of the original square template; we attribute the deformation of the structure to the compression of the sample during microtome sectioning.[66] The compression can be minimized with the use of ultrasonic knives[67] and by the choice of an embedding material that minimizes compression.[68]

Fabrication of Complex Nanostructures by Manipulating and Stacking of Arrays of Nanostructures Embedded in Epoxy Films. The thin polymer slabs containing the embedded nanostructures have some mechanical strength and can be manipulated to fabricate certain types of arrays of nanostructures that are difficult to prepare by other methods. We demonstrate the stacking of multiple slabs into layers to form quasi-3D nanostructures and the suspension of these slabs above gaps etched into flat surfaces and the positioning on curved surfaces.

Positioning of Epoxy Films with Embedded Metal Nanostructures on Nonplanar Surfaces. An advantage of the nanoskiving technique is the ability to position (by hand, see Figure 2B,C) nanometer-sized features by manipulating the epoxy sections of millimeter size. We demonstrate the utility of this ability using two examples: the positioning of parallel gold nanowires over a micrometer-wide "truncated-V"-shaped trench and the generation of an array of gold U-shaped nanostructures on a curved surface. We fabricated 20-μm wide truncated-V-shaped trenches by etching (using a potassium hydroxide (KOH) etch at 70 °C) a Si(100) wafer patterned with parallel 20-μm lines with 20-μm separation by photolithography.[69] We refer to the trench as "truncated" because we stopped the KOH etch before the two (111) sidewalls intersected. Figure 8A is an SEM image demonstrating the capability to position an epoxy section

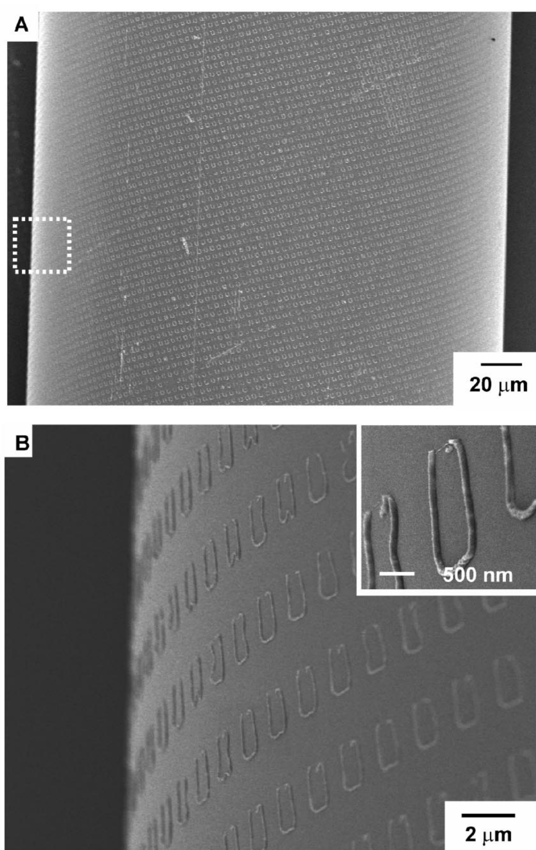

Figure 9. (A) SEM image of a 250-μm diameter glass rod with an array of U-shaped gold nanostructures positioned over the majority of the surface of the rod. (B) SEM image of the area outlined with the dotted white line in panel A. The inset is a magnified SEM image of the U-shaped gold nanostructures supported on the curved glass surface. In both images, we removed the epoxy with an oxygen plasma after positioning the epoxy section on the glass rod. A portion of the image in both panels is out of focus due to the curvature of the surface of the rod.

containing parallel gold nanowires over a series of parallel 20-μm-wide truncated-V-shaped trenches with 20-μm separation. After suspending the epoxy-embedded nanowires across the trench, we removed the epoxy with an oxygen plasma. The SEM image (rotated by 45°) in Figure 8B is of a single truncated-V-shaped trench with parallel gold nanowires draped over the trench. The inset of Figure 8B is a view of the nanowire near the sidewall of the trench. Figure 9A demonstrates the second example of positioning arrays of gold U-shaped nanostructures (Figure 7) embedded in an epoxy slab onto a 250-μm diameter pulled glass rod. Figure 9B is an SEM image of an array of U-shaped gold nanostructures situated on the curved surface of the glass rod outlined in Figure 9A. The inset of Figure 9B is an image of U-shaped nanostructures supported on the curved glass surface. After supporting the epoxy-embedded U-shaped nanostructures on the curved surface, we removed the epoxy with an oxygen plasma. The patterning of curved surfaces is difficult with both conventional photolithography and scanning-probe lithography but easily achieved with manual manipulation and positioning of nanostructures embedded in epoxy thin-film slabs produced by nanoskiving.

Stacking of the Thin Epoxy Sections To Form Quasi-3D Nanostructures. Figure 10A outlines the procedure we used to construct multilayer structures by stacking slabs on top of each other. Figure 10B is an SEM image of the resulting stacked sample. The first layer is an array of U-shaped gold nanostructures. Briefly, we selectively deposited 50 nm of gold by shadow evaporation on three sides of an array of square posts by electron-beam evaporation (Figure 7). We embedded metallic arrays in more epoxy and sectioned with an ultramicrotome to generate epoxy slabs with embedded U-shaped nanostructures. We transferred a 100-nm thick epoxy slab containing U-shaped nanostructures onto a TEM grid (70 mesh). After drying at room temperature, we stacked a second piece of 200-nm thick epoxy (without metal nanostructures) on top of the epoxy slab with embedded U-shaped nanostructures. We dried the two-layer sample in air for 5 min and then immersed the TEM grid in water and captured a 100-nm thick epoxy slab containing embedded parallel 2-μm lines (Figure 4B). We allowed this three-layer stack to dry and then used it in optical studies. Using only the stereomicroscope attached to the ultramicrotome, exact alignment of top and bottom layer is difficult to achieve since it is done manually.

Figure 10C is the transmission spectra of the stacked multilayer nanostructures and the individual films of epoxy-embedded nanostructures. In a separate publication, we studied in detail the transmission spectra of arrays of U-shaped nanostructures with experimental measurements and electrodynamic simulation.[53] Here, we collected the spectrum of the epoxy substrate separately and subtracted it from the spectrum of the array of U-shaped nanostructures, the array of parallel nanowires, and the stacked structure. The mid-IR transmission spectrum of the array of U-shaped nanostructures had three resonant peaks (5.1, 6.5, and 14.5 μm); we attribute these resonances to first-order and harmonic resonant plasmon modes induced by the unpolarized incident infrared light.[53] The transmission spectrum of a single epoxy slab (100-nm thickness) containing periodic parallel lines had no resonant peaks, and the transmission decreased continuously in the 4–16 μm region. This behavior is typical of a mid-IR wire-grid polarizer.[70] The transmission spectrum of the stacked multilayer assembly has a significantly more asymmetric lineshape than the transmission spectra of the array of the U-shaped nanostructures, with a single resonant peak at ~7 μm, which is red-shifted from the 6.5 μm peak observed with the U-shaped nanostructures. The parallel wires on top of the U-shaped nanostructures act as a polarizer, attenuating the two reso-

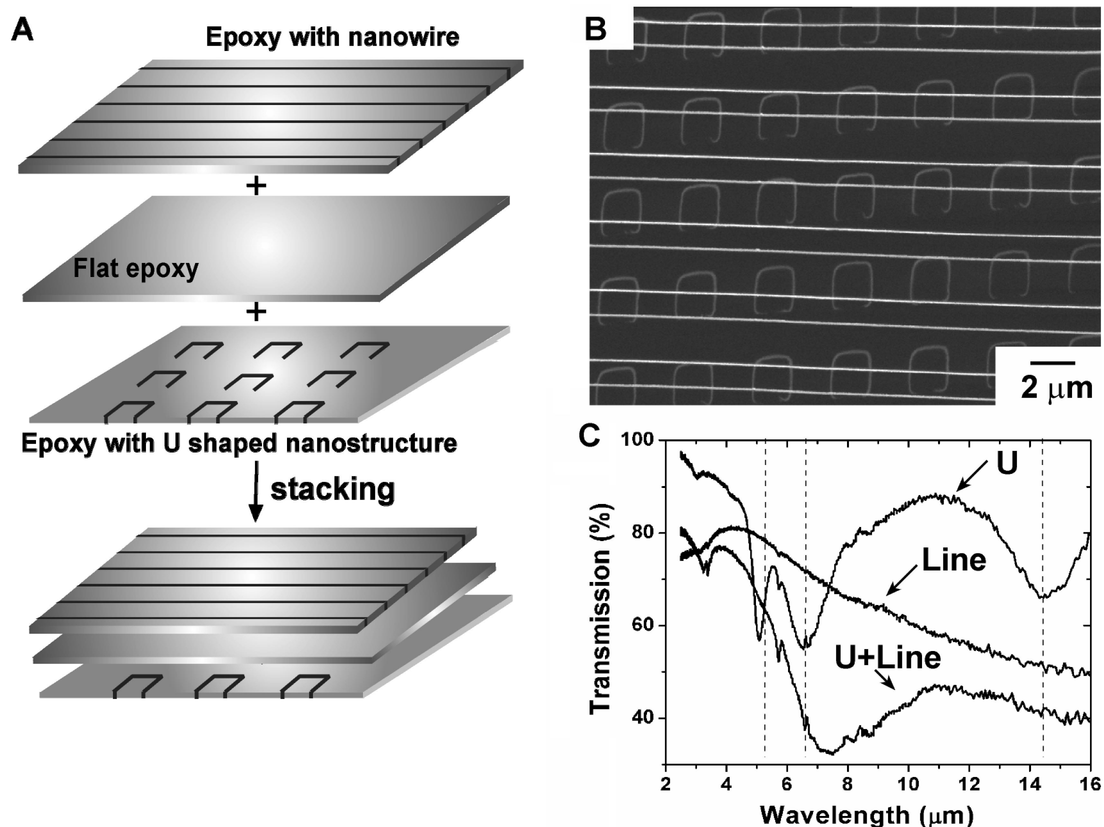

Figure 10. (A) Schematic illustration of the procedure for constructing multilayer structures by the stacking of multiple sections. The bottom layer of epoxy contains an array of U-shaped gold nanostructures (50 nm (*y*) × 100 nm (*z*)). We stacked a second section of epoxy (200 nm thick with no embedded nanostructures) on top of the epoxy slab containing the U-shaped nanostructures, followed by a third layer containing parallel gold nanowires (50 nm (*y*) × 100 nm (*z*)) on top of the blank epoxy film. (B) SEM image of the stacked, epoxy-embedded multilayer structure. The epoxy is essentially transparent to the electron beam and has minimal contrast in SEM. (C) Mid-IR transmission spectra of the individual elements and multilayer structure embedded in epoxy. The transmission spectrum of the parallel gold nanowires was featureless over this wavelength. The array of nanowires behaved as a wire-grid polarizer. The transmission spectrum of the array of U-shaped structures in the mid-infrared has three resonances located at 5.1, 6.5, and 14.5 μm, respectively. The array produced by stacking the U-shaped array on the parallel wire array had a transmission spectrum in which the peaks from the U-shaped spectra at 5.1 and 14.5 μm are attenuated completely and the lineshape of the remaining resonance is significantly more asymmetric and red-shifted.

nant peaks excited by the incident p-polarized light. These optical characteristics are consistent with our recent experimental results describing the behavior of arrays of U-shaped nanostructures irradiated by polarized IR light.[53] In this case, we inserted a commercial wire-grid polarizer in the path of the unpolarized incident mid-IR light in order to generate light with a single polarization.

CONCLUSIONS

This paper describes nanoskiving—the cutting of thin sections using an ultramicrotome—as a method to generate nanostructures. Nanoskiving provides a simple, convenient, and low-cost method to fabricate nanowires, nanoparticles, or certain kinds of more complex nanostructures. This fabrication technique needs only the readily available facilities required for replica molding, metal deposition (by e-beam or sputtering, depending on the application), and microtomy. Nanoskiving is compatible with a variety of materials, including inorganics (metals, semiconductors, and ceramics) and organic polymers. It is easily applicable to the fabrication of nanostructures with high aspect ratios (10); these structures are complementary to those fabricated by e-beam writing methods, which favor low-aspect-ratio structures.

The inclusion of these nanostructures in a mechanically stable matrix of epoxy allows them to be positioned, folded, rolled, stacked, and draped in ways that cannot be accomplished by other techniques. A range of polymers—including those with optical or electrical function—can, in principle, also be used as matrices; the only requirements are appropriate physical properties and adhesion to the metal thin film.

Nanoskiving substitutes "sectioning by microtome" for the "exposure" which is the pattern-transfer step in photolithography, "writing" in e-beam lithography and scanning-probe lithography, and "printing/molding" in soft lithography. Nanoskiving can serve as a method for *both* mastering and replicating arrays of nanostructures; in the role of a mastering technology, it is related—albeit distantly—to e-beam or scanning-probe

ARTICLE

lithography; in the role of a replicating technology, it has some analogy to photolithography or soft lithography. The versatility of nanoskiving—as a technique for both mastering and replicating—is not found in any of the other methods used for nanofabrication.

We believe this technique will be of primary interest to researchers who wish to generate simple nanostructures, singly or in arrays, more simply and quickly than can be accomplished by conventional means. It is easily accessible to those not trained in top-down procedures for fabrication and by those with limited or no access to the equipment and facilities needed for photolithography or scanning-beam fabrication.[71,72] In particular, this technique might especially appeal to biophysicists, because they are already familiar with microtomy (for the production of thin sections of biological matter for analysis by electron microscopy), and to optical physicists, since the structures of interest in optics often can tolerate a certain number of defects (electronic circuits typically cannot).

Nanoskiving has the potential to replace conventional microfabrication techniques for generating simple test structures in photonics. We demonstrated an example of a representative optical structure by stacking multiple epoxy sections containing metallic nanostructures; this structure is a mid-IR frequency-selective surface.

Nanoskiving has, of course, important limitations. It is currently restricted to generating unconnected line structures. The inability to fabricate connected structures limits the application of these nanostructures in making integrated circuits. The sectioning procedure leads to the introduction of artifacts and defects in the nanostructures. The compression of the sample during sectioning causes the true thickness of the individual nanostructure or individual elements in the array of nanostructures to be greater than the nominal thickness. Nanoskiving also does not currently have the stability in the pattern necessary to generate sections that can be registered precisely. We have—in the survey work described here—manipulated the sections by hand only with the aid of a stereomicroscope; the exact registration between multiple slabs in a stack is consequently poor. The distortion of the nanostructure limits our ability to stack slabs precisely; the importance of this distortion will depend on the particular application.

We believe the formation of more complex nanostructures will result from a combination of nanoskiving with other—conventional and unconventional—nanofabrication techniques. The large areas of pattern transfer achievable with photolithography (~square inches) and NIL (~square inches) are challenging for nanoskiving, because the knife can only cut square millimeter areas in each section. Generation of larger areas by nanoskiving required tiling of multiple smaller sections. The ability of capillary interaction to cause sections to self-assemble has the potential to assist in this kind of tiling.

We believe that many of the limitations of nanoskiving reflect the early stages of its development and that, as the technique develops, solutions to at least some of the current limitations will emerge.

EXPERIMENTAL SECTION

Fabrication of Flat and Patterned PDMS Molds. We obtained flat poly(dimethylsiloxane) (PDMS) surfaces by curing PDMS against an unsilanized polystyrene Petri dish. We obtained a topographically patterned PDMS master by molding PDMS against a photoresist patterned SiO_2/Si(100) substrate fabricated by conventional photolithography and standard procedures of soft lithography.[14] Typically, we coated a 2-μm thick layer of SU-8 5 photoresist (MicroChem Corp., Newton, MA) on silicon wafers (⟨100⟩, N/phosphorus or P/boron doped, 1–10 Ω-cm, Silicon Sense, Nashua, NH) by spin-coating the prepolymer at 3000 rpm for 30 s and processed according to manufacturer's specifications. We patterned the film of SU-8 with 2-μm lines with 2-μm separation using the corresponding chrome mask by photolithography, coated the surface with a release layer (tridecafluorotetrahydrooctyltrichorosilane, United Chemical Technologies, Bristol, PA), and molded with PDMS (Dow Corning Sylgard 184 kit, catalyst and prepolymer in 1:10 w/w ratio). The PDMS mold was cured for 3 h at 70 °C in a convection oven.

Fabrication of Flat and Patterned Epoxy Substrates. We cured an epoxy prepolymer (Araldite 502, Electron Microscopy Sciences, Fort Washington, PA) against a flat or patterned PDMS substrate at 70 °C for 12 h. Preparation of the epoxy required mixing the different kit components in the following amounts: 5 mL of diglycidyl ether of bisphenol-A (isopropylidenediphenol, Araldite 502), 5.5 mL of dodecenylsuccinic anhydride (DDSA), and 0.3 mL of benzyldimethylamine (BDMA).

Deposition of Metal and Dielectric Layers on Epoxy Surfaces. We deposited thin films of gold on flat or patterned epoxy surfaces by e-beam evaporation or sputtering. Gold was deposited at a rate of 1–3 Å/s by e-beam evaporation with the sample mounted on a rotating stage (30 rpm). We deposited the multilayer Au/SiO_2 films by sputtering (Orion Sputtering System, AJA International Inc., Scituate, MA) and deposited gold at a rate of 3.3 Å/s using a DC gun, and SiO_2 at a rate of 0.22 Å/s using an RF gun. We etched the SiO_2 layer with CF_4 (15 mTorr CF_4, 15 sccm CF_4, 200 W microwave, 200 W RF) for 30 s using a RIE system (Cirrus 150, Nexx Systems, Inc., Billerica, MA).

Fabrication of Au Nanoparticles by Shadow Deposition and Annealing. A commercial diffraction grating (1200 grooves/mm, Edmund Industrial Optics, Barrington, NJ) was silanized with 1*H*,1*H*,2*H*,2*H*-perfluorooctyltrichlorosilane (Fluka, 98%) overnight under house vacuum and replicated in PDMS according to standard soft lithography procedures.[14] We cured the PDMS mold at 70 °C for 3 h and separated the PDMS replica from the diffraction grating. After replication of the diffraction grating in epoxy by casting epoxy prepolymer against the PDMS replica and curing, we evaporated 10 nm of gold directly onto the epoxy replica by shadow evaporation with the sample mounted 70° from the plane for line-of-sight evaporation. The Au-coated epoxy replica was re-embedded in epoxy and cured overnight.

Microtome Sectioning. We placed the Au-coated epoxy film (planar or patterned) into a flat-embedding mold (Better Equipment For Electron Microscopy, Inc., West Chester, PA) (5.5 mm width × 12 mm length × 2.5 mm height) made of polyethylene, re-embedded in the same epoxy prepolymer, and cured at 70 °C overnight in a convection oven. We initially trimmed ("rough sectioning") the metal-film embedded epoxy block with

a razor blade to an area of ~0.5 mm × 0.5 mm with the aid of the stereomicroscope on the ultramicrotome (Leica Ultracut UCT, Leica, Inc., Germany) to expose a metal edge.[40] The surface created with the razor blade was smoothed using a glass knife before final sectioning with a diamond knife (Diatome Ultra 45°). After aligning the flat mold face with the diamond knife edge,[53] we sliced (0.5 mm/s sectioning speed) epoxy thin-film sections and collected the epoxy sections on the surface of the water contained in the sample trough mounted to the backside of the diamond knife. We directly immersed the solid substrate (such as TEM grid or silicon wafer) into water below the epoxy slab and pulled it toward the surface in a way that allowed the floating epoxy film to settle on it. Alternately, we trapped the epoxy slab on a thin film of water with a 2-mm diameter loop (Diatome Perfect Loop, Hatfield, PA) and deposited it on a chosen substrate by contacting the loop with the substrate and wicking away excess water with a paper tissue. We removed the epoxy embedding the metallic nanostructures by oxygen plasma (250–1000 mTorr O_2, 70 W barrel etcher, Anatech LTD, Alexandria, VA). The amount of time required for complete removal of epoxy depended on the thickness of the section: for example, a 50-nm-thick slab required 300 s for complete removal of the epoxy.

Optical Measurement. We used a Nicolet Fourier-transform infrared spectrometer in transmission mode to optically characterize the sample. We placed a piece of aluminum foil (~20 μm thick) with a punched hole (~1.5-mm diameter) directly in front of the sample. For all transmittance measurements, 128 scans with a resolution of 4 cm^{-1} were averaged. A separate spectrum of the clean substrate was collected and used as a reference. The transmittance spectrum of the frequency-selective surface was obtained by normalizing it to this reference.

SEM and Light Microscopy Imaging. We observed the nanostructures by SEM measurements using a LEO 982 SEM operating at 2 kV and a working distance of 2–6 mm, and by bright-field and dark-field optical microscopy using a Leica DMRX upright microscope.

Atomic Force Microscopy. We collected images of the gold nanoparticles supported on SiO_2/Si(100) substrates in tapping mode on a Veeco (Digital Instruments) Dimension 3100 scanning probe microscope.

Sample Preparation for TEM Imaging. We transferred epoxy sections containing metal nanoparticles onto a DuraSiN film support TEM grid (DTF-1523, Electron Microscopy Sciences, Fort Washington, PA). After removing the epoxy with oxygen plasma, we heated the sample in a convection oven at 500 °C for 2 h in air. We measured the transmission spectrum and selected-area electron diffraction of the annealed gold nanoparticles using a Jeol 2100 TEM at an operating voltage of 200 kV.

Acknowledgment. This research was supported by NIH (GM065364) and by DARPA (sub-award to G.M.W. from the Center for Optofluidic Integration at the California Institute of Technology). We acknowledge the use of MRSEC and NSEC shared facilities supported by NSF under awards DMR-0213805 (MRSEC) and PHY-0117795 (NSEC). This work was performed in part at the Center for Nanoscale Systems (CNS), a member of the National Nanotechnology Infrastructure Network (NNIN), which is supported by the National Science Foundation under NSF award no. ECS-0335765. CNS is part of the Faculty of Arts and Sciences at Harvard University. R.M.R. acknowledges the support of the National Institute of Health (NIH) in the form of a postdoctoral fellowship (1 F32 NS060356). We thank Dr. Richard Schalek of the CNS at Harvard University for help with microtome sectioning and Hongtao Wang of Harvard University for help with TEM. We thank Dr. Jiming Bao of the School of Engineering and Applied Science at Harvard University for helpful discussion about the mid-IR transmission measurement. We acknowledge Dr. Helmut Gnägi of Diatome for private communication concerning suitable materials for ultramicrotome sectioning at room temperature. We acknowledge Dr. Reinhard Lihl of Leica Microsystems for private communication concerning the design of an ultramicrotome.

Supporting Information Available: Supporting Figures S1–S3. This material is available free of charge *via* the Internet at http://pubs.acs.org.

REFERENCES AND NOTES

1. According to the Merriam-Webster dictionary, the verb "to skive" is of Scandinavian origin and defined as "to cut off in thin layers or pieces". It is often used in the context of cutting rubber or leather.
2. Brainard, R. L.; Cobb, J.; Cutler, C. A. Current Status of EUV Photoresists. *J. Photopolym. Sci. Technol.* **2003**, *16*, 401–410.
3. Cerrina, F.; Bollepalli, S.; Khan, M.; Solak, H.; Li, W.; He, D. Image Formation in EUV Lithography: Multilayer and Resist Properties. *Microelectron. Eng.* **2000**, *53*, 13–20.
4. Goethals, A. M.; Bisschop, P. D.; Hermans, J.; Jonckheere, R.; Van Roey, F.; Van den Heuvel, D.; Eliat, A.; Ronse, K. Introducing 157 nm Full Field Lithography. *J. Photopolym. Sci. Technol.* **2003**, *16*, 549–556.
5. Mulkens, J.; McClay, J.; Tirri, B.; Brunotte, M.; Mecking, B.; Jasper, H. Optical Lithography Solutions for Sub-65 nm Semiconductor Devices. *Proc. SPIE–Int. Soc. Opt. Eng.* **2003**, *5040*, 753–762.
6. Gamo, K. Nanofabrication by FIB. *Microelectron. Eng.* **1996**, *32*, 159–171.
7. Huang, W.-S.; He, W.; Li, W.; Moreau, W. M.; Lang, R.; Medeiros, D. R.; Petrillo, K. E.; Mahorowala, A. P.; Angelopoulos, M.; Deverich, C.; *et al.* Current Developments of a High-Performance CA Resist for Mask-Making Application. *Proc. SPIE–Int. Soc. Opt. Eng.* **2003**, *5130*, 58–66.
8. Kubena, R. L. Resolution Limits of Focused-Ion-Beam Resist Patterning. *Mater. Res. Soc. Symp. Proc.* **1993**, *279*, 567–576.
9. Yasin, S.; Hasko, D. G.; Ahmed, H. Fabrication of <5 nm Width Lines in Poly(methyl methacrylate) Resist using a Water:Isopropyl Alcohol Developer and Ultrasonically-Assisted Development. *Appl. Phys. Lett.* **2001**, *78*, 2760–2762.
10. Li, L.; Fourkas, J. T. Multiphoton Polymerization. *Mater. Today* **2007**, *10*, 30–37.
11. Xia, Y.; Rogers, J. A.; Paul, K. E.; Whitesides, G. M. Unconventional Methods for Fabricating and Patterning Nanostructures. *Chem. Rev.* **1999**, *99*, 1823–1848.
12. Gates, B. D.; Xu, Q.; Love, J. C.; Wolfe, D. B.; Whitesides, G. M. Unconventional Nanofabrication. *Annu. Rev. Mater. Res.* **2004**, *34*, 339–372.
13. Gates, B. D.; Xu, Q.; Stewart, M.; Ryan, D.; Willson, C. G.; Whitesides, G. M. New Approaches to Nanofabrication: Molding, Printing, and Other Techniques. *Chem. Rev.* **2005**, *105*, 1171–1196.
14. Xia, Y.; Whitesides, G. M. Soft Lithography. *Angew. Chem., Int. Ed.* **1998**, *37*, 550–575.
15. Kumar, A.; Whitesides, G. M. Features of Gold Having Micrometer to Centimeter Dimensions Can be Formed Through a Combination of Stamping with an Elastomeric Stamp and an Alkanethiol "Ink" Followed by Chemical Etching. *Appl. Phys. Lett.* **1993**, *63*, 2002–2004.
16. Kim, E.; Xia, Y.; Whitesides, G. M. Polymer Microstructures Formed by Molding in Capillaries. *Nature* **1995**, *376*, 581–584.
17. Xia, Y.; Whitesides, G. M. Use of Controlled Reactive Spreading of Liquid Alkanethiol on the Surface of Gold To Modify the Size of Features Produced by Microcontact Printing. *J. Am. Chem. Soc.* **1995**, *117*, 3274–3275.
18. Xia, Y.; Kim, E.; Zhao, X.-M.; Rogers, J. A.; Prentiss, M.; Whitesides, G. M. Complex Optical Surfaces Formed by Replica Molding Against Elastomeric Masters. *Science* **1996**, *273*, 347–349.
19. Biebuyck, H. A.; Larsen, N. B.; Delamarche, E.; Michel, B. Lithography Beyond Light: Microcontact Printing with Monolayer Resists. *IBM J. Res. Dev.* **1997**, *41*, 159–170.
20. Kim, E.; Xia, Y.; Zhao, X. M.; Whitesides, G. M. Solvent-Assisted Microcontact Molding: A Convenient Method for Fabricating Three-Dimensional Structures on Surfaces of Polymers. *Adv. Mater.* **1997**, *9*, 651–654.

21. Xia, Y.; McClelland, J. J.; Gupta, R.; Qin, D.; Zhao, X. M.; Sohn, L. L.; Celotta, R. J.; Whitesides, G. M. Replica Molding Using Polymeric Materials: A Practical Step Toward Nanomanufacturing. *Adv. Mater.* **1997**, *9*, 147–149.
22. Delamarche, E.; Geissler, M.; Wolf, H.; Michel, B. Positive Microcontact Printing. *J. Am. Chem. Soc.* **2002**, *124*, 3834–3835.
23. Geissler, M.; Schmid, H.; Bietsch, A.; Michel, B.; Delamarche, E. Defect-Tolerant and Directional Wet-Etch Systems for Using Monolayers as Resists. *Langmuir* **2002**, *18*, 2374–2377.
24. Loo, Y.-L.; Hsu, J. W. P.; Willett, R. L.; Baldwin, K. W.; West, K. W.; Rogers, J. A. High-Resolution Transfer Printing on GaAs Surfaces Using Alkane Dithiol Monolayers. *J. Vac. Sci. Technol. B* **2002**, *20*, 2853–2856.
25. Love, J. C.; Wolfe, D. B.; Chabinyc, M. L.; Paul, K. E.; Whitesides, G. M. Self-Assembled Monolayers of Alkanethiolates on Palladium Are Good Etch Resists. *J. Am. Chem. Soc.* **2002**, *124*, 1576–1577.
26. Zaumseil, J.; Meitl, M. A.; Hsu, J. W. P.; Acharya, B. R.; Baldwin, K. W.; Loo, Y.-L.; Rogers, J. A. Three-Dimensional and Multilayer Nanostructures Formed by Nanotransfer Printing. *Nano Lett.* **2003**, *3*, 1223–1227.
27. Love, J. C.; Estroff, L. A.; Kriebel, J. K.; Nuzzo, R. G.; Whitesides, G. M. Self-Assembled Monolayers of Thiolates on Metals as a Form of Nanotechnology. *Chem. Rev.* **2005**, *105*, 1103–1169.
28. Zhao, X. M.; Xia, Y.; Whitesides, G. M. Fabrication of Three-Dimensional Microstructure: Microtransfer Molding. *Adv. Mater.* **1996**, *8*, 837–840.
29. Martin, C. R. Nanomaterials: A Membrane-Based Synthetic Approach. *Science* **1994**, *266*, 1961–1966.
30. Smith, P. A.; Nordquist, C. D.; Jackson, T. N.; Mayer, T. S.; Martin, B. R.; Mbindyo, J.; Mallouk, T. E. Electric-Field Assisted Assembly and Alignment of Metallic Nanowires. *Appl. Phys. Lett.* **2000**, *77*, 1399–1401.
31. Chou, S. Y.; Krauss, P. R.; Renstrom, P. J. Nanoimprint Lithography. *J. Vac. Sci. Technol. B* **1996**, *14*, 4129–4133.
32. Chou, S. Y.; Krauss, P. R.; Renstrom, P. J. Imprint Lithography with 25-Nanometer Resolution. *Science* **1996**, *272*, 85–87.
33. Chou, S. Y.; Krauss, P. R.; Zhang, W.; Guo, L.; Zhuang, L. Sub-10 nm Imprint Lithography and Applications. *J. Vac. Sci. Technol. B* **1997**, *15*, 2897–2904.
34. Wu, W.; Yu, Z. N.; Wang, S. Y.; Williams, R. S.; Liu, Y. M.; Sun, C.; Zhang, X.; Kim, E.; Shen, Y. R.; Fang, N. X. Midinfrared Metamaterials Fabricated by Nanoimprint Lithography. *Appl. Phys. Lett.* **2007**, *90*, 063107.
35. Resnick, D. J.; Dauksher, W. J.; Mancini, D. P.; Nordquist, K. J.; Ainley, E. S.; Gehoski, K. A.; Baker, J. H.; Bailey, T. C.; Choi, B. J.; Johnson, S.; *et al. Proc. SPIE–Int. Soc. Opt. Eng.* **2002**, *4688*, 205–213.
36. Colburn, M.; Grot, A.; Amistoso, M. N.; Choi, B. J.; Bailey, T. C.; Ekerdt, J. G.; Sreenivasan, S. V.; Hollenhorst, J.; Willson, C. G. Step and Flash Imprint Lithography for Sub-100-nm Patterning. *Proc. SPIE–Int. Soc. Opt. Eng.* **2000**, *3997*, 453–457.
37. Odom, T. W.; Thalladi, V. R.; Love, J. C.; Whitesides, G. M. Generation of 30–50 nm Structures Using Easily Fabricated, Composite PDMS Masks. *J. Am. Chem. Soc.* **2002**, *124*, 12112–12113.
38. Gates, B. D.; Xu, Q.; Thalladi, V. R.; Cao, T.; Knickerbocker, T.; Whitesides, G. M. Shear Patterning of Microdominos: A New Class of Procedures for Making Micro- and Nanostructures. *Angew. Chem., Int. Ed.* **2004**, *43*, 2780–2783.
39. Melosh, N. A.; Boukai, A.; Diana, F.; Gerardot, B.; Badolato, A.; Petroff, P. M.; Heath, J. R. Ultrahigh-Density Nanowire Lattices and Circuits. *Science* **2003**, *300*, 112–115.
40. Xu, Q.; Gates, B. D.; Whitesides, G. M. Fabrication of Metal Structures with Nanometer-Scale Lateral Dimensions by Sectioning Using a Microtome. *J. Am. Chem. Soc.* **2004**, *126*, 1332–1333.
41. Aizenberg, J.; Black, A. J.; Whitesides, G. M. Controlling Local Disorder in Self-Assembled Monolayers by Patterning the Topography of their Metallic Supports. *Nature* **1998**, *394*, 868–871.
42. Cao, T. B.; Xu, Q. B.; Winkleman, A.; Whitesides, G. M. Fabrication of Thin, Metallic Films Along the Sidewalls of a Topographically Patterned Stamp and their Application in Charge Printing. *Small* **2005**, *1*, 1191–1195.
43. Crommie, M. F.; Lutz, C. P.; Eigler, D. M. Confinement of Electrons to Quantum Corrals on a Metal Surface. *Science* **1993**, *262*, 218–220.
44. Dagata, J. A.; Schneir, J.; Harary, H. H.; Evans, C. J.; Postek, M. T.; Bennett, J. Modification of Hydrogen Passivated Silicon by a Scanning Tunneling Microscope Operating in Air. *Appl. Phys. Lett.* **1990**, *56*, 2001–2003.
45. Ginger, D. S.; Zhang, H.; Mirkin, C. A. The Evolution of Dip-Pen Nanolithography. *Angew. Chem., Int. Ed.* **2004**, *43*, 30–35.
46. Liu, G.-Y.; Xu, S.; Qian, Y. Nanofabrication of Self-Assembled Monolayers Using Scanning Probe Lithography. *Acc. Chem. Res.* **2000**, *33*, 457–466.
47. Wouters, D.; Schubert, U. S. Nanolithography and Nanochemistry: Probe-Related Patterning Techniques and Chemical Modification for Nanometer-Sized Devices. *Angew. Chem., Int. Ed.* **2004**, *43*, 2480–2495.
48. Hong, S. H.; Mirkin, C. A. A Nanoplotter with Both Parallel and Serial Writing Capabilities. *Science* **2000**, *288*, 1808–1811.
49. Piner, R. D.; Zhu, J.; Xu, F.; Hong, S.; Mirkin, C. A. "Dip-Pen" Nanolithography. *Science* **1999**, *283*, 661–663.
50. Zhang, H.; Mirkin, C. A. DPN-Generated Nnanostructures Made of Gold, Silver, and Palladium. *Chem. Mater.* **2004**, *16*, 1480–1484.
51. Salaita, K.; Wang, Y. H.; Mirkin, C. A. Applications of Dip-Pen Nanolithography. *Nature Nanotechnol.* **2007**, *2*, 145–155.
52. Xu, Q.; Bao, J.; Capasso, F.; Whitesides, G. M. Surface Plasmon Resonances of Free-Standing Gold Nanowires Fabricated by Nanoskiving. *Angew. Chem., Int. Ed.* **2006**, *45*, 3631–3635.
53. Xu, Q.; Bao, J.; Rioux, R. M.; Perez-Castillejos, R.; Capasso, F.; Whitesides, G. M. Fabrication of Large-Area Patterned Nanostructures for Optical Applications by Nanoskiving. *Nano Lett.* **2007**, *7*, 2800–2805.
54. Xu, Q. B.; Perez-Castillejos, R.; Li, Z. F.; Whitesides, G. M. Fabrication of High-Aspect-Ratio Metallic Nanostructures Using Nanoskiving. *Nano Lett.* **2006**, *6*, 2163–2165.
55. According to Random House Unabridged dictionary, the noun "microtomy" is the process of cutting of very thin sections with a microtome.
56. Glauert, A. M. *Practical Methods in Electron Microscopy*; American Elsevier Publishing Co. Inc.: New York, 1974.
57. Plummer, H. K. Reflections on the Use of Microtomy for Materials science Specimen Preparation. *Microsc. Microanal.* **1997**, *3*, 239–260.
58. The details of operation of a microtome are proprietary. This information was kindly provided by Dr. R. Lihl, R&D manager at Leica Microsystems.
59. Butler, J. K. Methods for Improved Light Microscope Microtomy. *Stain Technol.* **1979**, *54*, 53–69.
60. http://www.emsdiasum.com/Diatome/diamond_knives/default.htm.
61. Glauert, A. M.; Rogers, G. E.; Glauert, R. H. New Embedding Medium for Electron Microscopy. *Nature* **1956**, *178*, 803–803.
62. Glauert, A. M.; Glauert, R. H. Araldite as an Embedding Medium for Electron Microscopy. *J. Biophys. Biochem. Cytlo.* **1958**, *4*, 191–194.
63. A thin layer of Ti (2 nm) improved the adhesion between the epoxy and gold.
64. Peachey, L. D. Thin Sections. 1. A Study of Section Thickness and Physical Distortion Produced During Microtomy. *J. Biophys. Biochem. Cytol.* **1958**, *4*, 233–242.
65. Blumer, M. J. F.; Gahleitner, P.; Narzt, T.; Handl, C.; Ruthensteiner, B. Ribbons of Semithin Sections: An Advanced Method with a New Type of Diamond Knife. *J. Neurosci. Methods* **2002**, *120*, 11–16.

66. Richter, K. Cutting Artifacts on Ultrathin Cryosections of Biological Bulk Specimens. *Micron* **1994**, *25*, 297–308.
67. Studer, D.; Gnaegi, H. Minimal Compression of Ultrathin Sections with Use of an Oscillating Diamond Knife. *J. Microsc.* **2000**, *197*, 94–100.
68. Private communication with Dr. Helmut Gnägi, Diatome Ltd., Biel, Switzerland.
69. Xu, Q. B.; Tonks, I.; Fuerstman, M. J.; Love, J. C.; Whitesides, G. M. Fabrication of Free-Standing Metallic Pyramidal Shells. *Nano Lett.* **2004**, *4*, 2509–2511.
70. Baba, K.; Shiraishi, K.; Obi, K.; Kataoka, T.; Kawakami, S. Optical Properties of Very Thin Metal-Films for Laminated Polarizers. *Appl. Opt.* **1988**, *27*, 2554–2560.
71. Cavalcanti-Adam, E. A.; Volberg, T.; Micoulet, A.; Kessler, H.; Geiger, B.; Spatz, J. P. Cell Spreading and Focal Adhesion Dynamics are Regulated by Spacing of Integrin Ligands. *Biophys. J.* **2007**, *92*, 2964–2974.
72. Mossman, K. D.; Campi, G.; Groves, J. T.; Dustin, M. L. Altered TCR Signaling from Geometrically Repatterned Immunological Synapses. *Science* **2005**, *310*, 1191–1193.